Dynamics of a Supersonic Plume Moving along a Magnetized Plasma

F. S. Tsung, G. J. Morales, and J. N. Leboeuf

Department of Physics and Astronomy, University of California–Los Angeles, Los Angeles, California 90095

(Received 15 August 2002; published 6 February 2003)

A particle-in-cell code is used to investigate the evolution of a density plume moving through a background plasma with supersonic speed directed along the confinement magnetic field. For scale lengths representative of laboratory and auroral phenomena, the major nonlinear effects identified by the present simulations are the formation of a bipolar current system from the ballistic electrons, the appearance of transient potential layers, and the carving of deep density cavities. A 3D magnetic topology is generated by the self-consistent ballistic and diamagnetic currents that accompany highly localized potential layers.

DOI: 10.1103/PhysRevLett.90.055004 PACS numbers: 52.30.–q, 52.35.Tc, 52.65.Rr

The motion of a dense plasma plume (or filament) along an ambient magnetized plasma is a phenomenon that arises in a wide range of natural and controlled environments. Events of this type are a by-product of mass ejections in the solar corona [1], give rise to structures in the solar wind [2], and can play a role in the formation of features sampled by spacecrafts [3,4]. Plumes can be generated in the laboratory by laser ablation of solid targets [5,6] and have a broad range of technological applications. Recently, the expansion of a supersonic plume in a large magnetized plasma has been observed [7] to generate large amplitude Alfvén waves. In general, the localized release of substantial energy generates moving plasma plumes.

This study focuses on issues related to kinetic processes that cause nonlocal modifications in the ambient plasma. These events lead to energy and mass transport as well as to the formation of long-lived current and density structures. This perspective is also pursued in magnetic confinement studies [8]. As a first step we investigate the behavior of plumes whose extent across the magnetic field is comparable to the electron skin depth c/ω_p, where c is the speed of light and ω_p is the electron plasma frequency. The scales investigated here are more representative of laboratory studies [7] and of structures observed in the auroral ionosphere [9].

This study ignores the issue of how the initial plume is generated. Although this is an important topic, it detracts from the immediate goal, i.e., to identify the major nonlinear processes. We legislate the initial density, temperature, and speed of the plume and follow its space-time evolution as it propagates through a background plasma of uniform density and temperature. The choice of parameters is dictated by practical considerations set by the state-of-the art computing power.

This computational investigation uses an electromagnetic, particle-in-cell code that is based on an object-oriented code (OSIRIS) originally developed at UCLA [10] to study relativistic laser-plasma interactions. The present configuration follows the relativistic, fully magnetized trajectories of ions and electrons. It has been verified that the code correctly simulates the linear properties of shear and compressional Alfvén waves of relevance to the electrodynamics of plume expansion. For the results reported the code is run in 2-1/2 dimensions, i.e., two spatial coordinates and three velocity coordinates. One of the coordinates across the confinement field is taken as ignorable and the other two are periodic. The periodicity length is chosen sufficiently large to approximate the response of a background plasma of infinite extent.

The ion to electron mass ratio used is $M/m = 20$ which implies that the ratio of the ion acoustic speed to the electron thermal velocity is $c_s/v_e = 0.22$. This allows for the practical separation of the relevant time scales within a run spanning several ion gyroperiods while retaining full electron dynamics. Realistic mass ratios have been used in previous PIC simulations [11,12] of plasma expansion into a vacuum, but the codes used have been one-dimensional, unmagnetized, and electrostatic. The ratio of the electron plasma frequency to the electron gyrofrequency is $\omega_p/\Omega_{ce} = 2.5$, the ratio of the electron thermal velocity to the speed of light is $v_e/c = 0.05$, and the Alfvén speed is $v_A/c = 0.097$. The ordering of the relevant speeds is $c \gg v_A > v_e \gg c_s$, which implies that the Alfvénic phenomena are in the inertial regime, i.e., the electron plasma beta parameter is $\beta_e = 2.5 \times 10^{-2}$ which is smaller than the mass ratio m/M. The dimensions of the simulation box are $L_z = 57c/\omega_{pe}$ along the magnetic field and $L_x = 20c/\omega_{pe}$ perpendicular to the field line. The results presented here are not sensitive to the box size, as has been checked by runs with a box twice as large as that indicated.

The initial density profile of the plume is $n_p(x, z) = n_p(0)\{1 - [(z - z_0)/\Delta_z]^2\}\{1 - [(x - x_0)/\Delta_x]^2\}$. The results described correspond to $\Delta_z = 5c/\omega_p$ and $\Delta_x = 0.5$ and $2c/\omega_p$, with plume peak densities equal to or twice as large as the density of the background plasma n_0. The coordinate system used is (x, y, z) with the confinement magnetic field B_0 pointing in the negative z direction, and

x is transverse to z with y the ignorable spatial coordinate. The plume is initialized with its center of mass velocity v_p directed along the magnetic field, i.e., towards the left in the figures presented. The axial position z_0 is chosen far to the right so that the late stages can be imaged in the figures. We consider the supersonic regime with $v_p = v_e$. The plume and background ions are initially cold while the plume and background electrons have equal and isotropic temperatures T_e in their respective rest frames. Thus, phenomena regulated by large ion Larmor radius effects are not sampled. In the figures the scaled time coordinate is $T = t\omega_p$, the axial and transverse coordinates are scaled to c/ω_p, and density to n_0.

A key feature in the expansion of a localized, plasma density enhancement is that the electrons move very rapidly out of the peak density and leave behind the more massive ions. If the expansion occurs into a vacuum region, an ambipolar electric field develops that holds the electrons back and results in a self-similar expansion, as has been documented in an early simulation [11] and also in a recent study [12]. In the latter, strong ion acceleration into the vacuum has been shown to occur, but not as large as has been predicted [13]. In contrast, we find that in the presence of a background plasma the outgoing electrons can be neutralized and a significant ballistic current develops. In this situation the induction electric field sets up a current system that closes on itself, a missing feature in electrostatic and/or MHD studies. This results in a macroscopic dipolar current that generates a quasistatic, perturbed magnetic field which is convected with the supersonic plume.

The following summarizes the behavior extracted from our simulations. The early stage ($t \approx \Delta_z/v_e$) consists of the ballistic outflow of electrons and formation of a region of large positive potential. The background ions are ejected rapidly across the magnetic field while the background electrons are trapped in the deep potential well anchored to the center of mass of the plume. If the plume remained stationary, an equilibrium would be reached leading to equalization of the pressure gradients at the sound speed. However, for a supersonic plume an equilibrium is not reached and within a time scale ($t \approx \Delta_z/2c_s$) comparable to the sound transit time across the axial gradient, a shock forms. Prior to shock formation it is found that the total ion density is well described quantitatively as a splitting sound pulse in the frame of the moving plume. Later on, fine scale structures develop within the leading edge of the moving plume and an oscillatory wake is formed. In the late stage ($t > 2\Delta_z/c_s$), an extended region of depleted density ($\delta n/n_0 \approx 0.3$) is formed behind a small number of plume ions that lose almost all of their initial energy. These processes are accompanied by the generation of perturbed magnetic fields along the three spatial coordinates.

The top panel in Fig. 1 displays a contour of the perturbed magnetic field component along the parallel z direction at a scaled time $T = 324$ ($T = 250$ corresponds to $t = \Delta_z/2c_s$) for a case with $\Delta_x = 0.5c/\omega_p$ and $n_p(0) = 2n_0$. Red corresponds to the largest positive value (pointing to the right) and dark blue to the largest negative value (pointing to the left). This component of the field is generated by diamagnetic currents along the y direction associated with the transverse pressure gradient. The total magnetic field is reduced inside the plume ($\delta B_z/B_0 \approx 0.035$) and it is enhanced above and below the location of the plume. The faint light trace ahead of the plume and along the center arises from the additional plasma pressure provided by the ballistic electrons. In essence they generate a dilute density filament shielded locally by cross-field currents due to background ions at a time much earlier than the arrival of the plume ions. Similar faint traces to the right of the figure indicate that multiple filaments appear in the wake region.

The bottom panel in Fig. 1 exhibits a contour of the total parallel current density at the same time as the diamagnetic field. Again, red corresponds to right-going currents and dark blue to left-going currents. The extended positive current ahead of the plume center is generated by the ballistic electrons going left. Surrounding the bright red channel there are two faint blue stripes (above and below) associated with the return currents driven by the induction field, i.e., a coaxial current system develops ahead of the plume. The dark blue region close to the axial location 30 in the horizontal axis, however, is not due to ballistic electrons because it is collocated with the peak pressure region seen in the top panel. This relatively large current density region (with $J_z \approx 0.1en_0v_e$) corresponds to a net positive charge

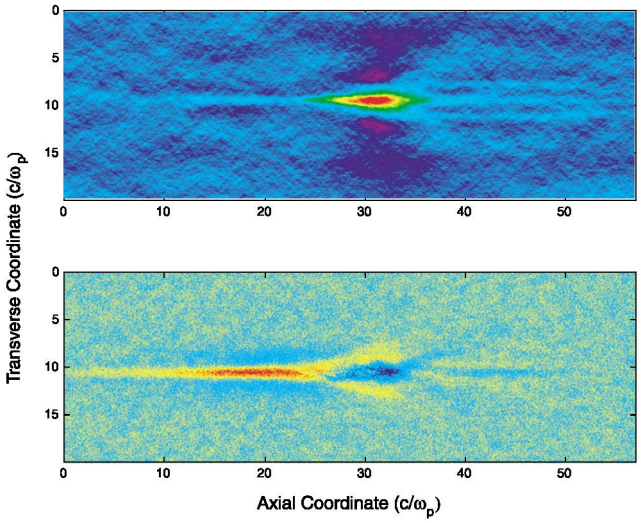

FIG. 1 (color). Two-dimensional color contours at an intermediate stage in evolution. Top panel: parallel component of magnetic field illustrating the plume diamagnetic effect. Bottom panel: parallel current density showing strong ballistic contribution. Red points to the right and blue to the left. Initial plume moves to the left along the confinement magnetic field.

moving to the left and experiencing its own coaxial shielding by background electrons at radial distances larger than Δ_x. The faint blue line well behind the plume (to the right in Fig. 1) corresponds to the right-going ballistic electrons.

To identify the spatial charge configuration associated with the dipolar parallel current density we examine the axial structure along the centerline of the plume ($x_0 = 10$), as shown in Fig. 2 for a case corresponding to $\Delta_x = 2c/\omega_p$ and $n_p(0) = n_0$ at the time $T = 378$. The black line is the predicted current density according to the linear ballistic theory. In this calculation the charges freely expand without self-consistent effects taken into consideration. The elongated positive segment to the left is due to the fast electrons moving (dispersing) in the same direction as the center of mass of the plume, while the smaller negative portion on the right is due to right-going fast electrons moving against the flow. The smaller and rounded negative dip near the center is due to the plume ions moving to the left. The red curve is the self-consistent, total current density obtained from the simulation. It is seen that the left-going electrons are not as dispersed as in the ballistic prediction. The front portion of the plume ions follows the ballistic prediction, but there is a large negative dip towards the rear whose magnitude exceeds the ballistic contribution. This indicates that a region of net positive charge is formed within the rear of the plume. Comparing the black and red curves to the right of Fig. 2 indicates that this excess positive charge significantly modifies the ballistic expansion of electrons in the wake of the plume, essentially causing a region of near zero current density immediately behind the plume and breaking into oscillations farther away. The blue curve in Fig. 2 is the density of plume ions (not the total density) and illustrates that a shock develops toward the rear of the plume. The region where shock compression occurs results in the locally nonneutral plasma that forms the negative portion of the moving dipolar current.

The top panel in Fig. 3 displays contours of the total ion density at a late time $T = 540$ for $\Delta_x = 0.5c/\omega_p$ and $n_p(0) = 2n_0$. Deep blue represents low values and red, large values of the density. It is seen that in the axial region between positions 15 and 30 multiple Machlike cones are present and they emanate from regions of local compression where there is charge imbalance and bipolar electric fields appear in a transient manner. The observed pattern is reminiscent of the Mach cones imaged in recent studies [14,15] of dusty plasmas, in which macroscopic charges are accelerated to supersonic speeds by a laser. In here the analogous phenomenon arises from the nonlinear dynamics of the plume expansion. The deep blue region between axial locations 32 and 42 indicates that the plume carves out a substantial density cavity that remains long after its passage. The bottom panel in Fig. 3 displays the corresponding ion density along the centerline ($x_0 = 10$). The density depression is now clearly seen to trail the plume. For comparison, the smooth curve corresponds to the linear theory prediction of a splitting sound pulse in the moving frame of the plume. It is seen that the plume dynamics washes out the forward-going pulse and it is suggestive that the backward pulse moves faster (to the right) than the linear, acoustic speed.

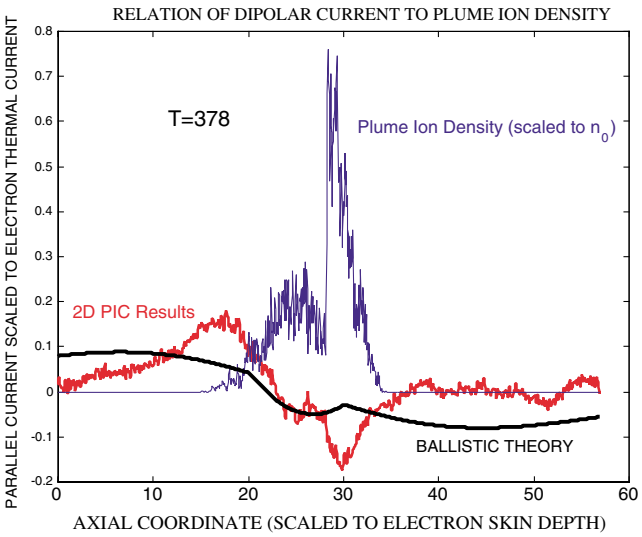

FIG. 2 (color). Axial dependence along the centerline of the plume showing the relation of dipolar current to plume density. The red curve is the simulation result, and black is ballistic theory prediction. The blue curve is the density of plume ions scaled to background density.

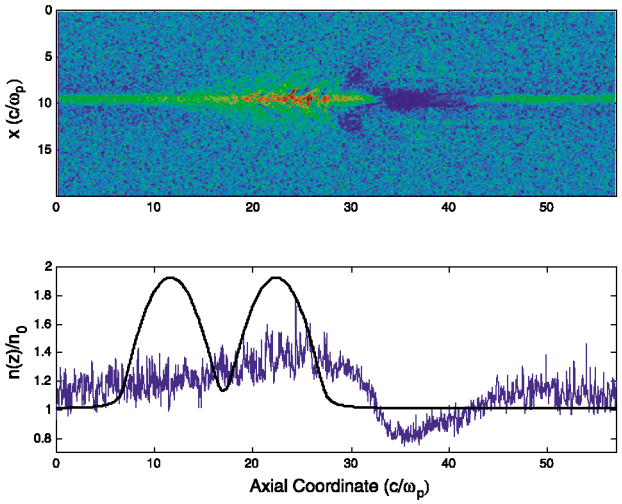

FIG. 3 (color). Top panel: a two-dimensional color contour of total ion density at a late stage in evolution showing multiple Mach cones and trailing density cavity. Red is higher density and blue lower. Bottom panel: Axial dependence of total density along the centerline. The noisy curve is the simulation result, and the solid curve is the linear prediction of acoustic pulse splitting.

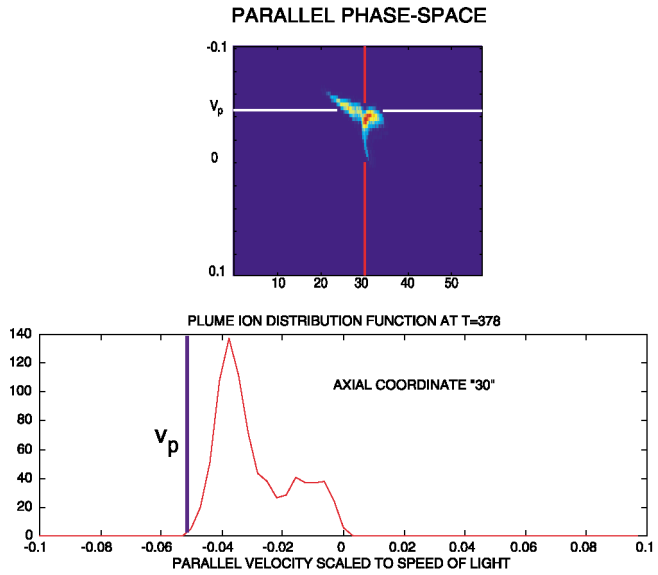

FIG. 4 (color). Top panel: color contour of parallel phase space (v_z, z) of plume ions at an intermediate stage showing streaming and strongly decelerated components. Dark blue is zero and red is the largest number density. Bottom panel: corresponding parallel velocity distribution projected along the red line above. The vertical line indicates initial distribution.

The parallel phase space of the plume ions is shown in the top panel of Fig. 4. In here dark blue corresponds to zero, and red to large phase-space density. The feature towards the upper left corner is characteristic of beam-like velocity dispersion, and is associated with the directed velocity of the original plume. The vertical portion indicates that a fraction of the plume undergoes substantial deceleration. This is best illustrated by projecting the ion velocity-distribution function at a fixed axial location (indicated by the red line) corresponding to the axial region in the bottom panel of Fig. 3 where the density appears to move against the flow faster than the ion acoustic speed. The result is shown in the bottom panel of Fig. 4. For reference the initial distribution function is represented by the solid vertical line. The main peak of the plume ions recoils by an amount close to the sound speed (i.e., $\Delta v_z/c \approx 0.01 = c_s/c$). This would correspond to the right-side lobe of the split pulse in the linear theory shown in the bottom panel of Fig. 3. In addition, a fraction of the ions is slowed more than this nominal value, and some are brought to rest in the lab frame. In order for this to occur, small-scale potential layers develop within the plume whose magnitude is on the order of $e\phi = Mv_p^2/2$ which implies for these parameters that $e\phi/T_e \approx 10$. It is noteworthy that this corresponds to the maximum ion energy change predicted [13] for expansion into vacuum.

The perspective achieved from this computer simulation study is that supersonic motion through a magnetized plasma is regulated by the ballistic expansion of the fast electrons initially in the plume. It is the current associated with these electrons and the resulting coaxial shielding by the background plasma that is likely [16] to be responsible for the efficient generation of Alfvén waves in a recent experimental study [7] of this phenomenon. Of course, in the laboratory finite boundaries are present that cause the additional excitation of field line resonances [17]. The major nonlinear effects identified by the present simulations are the formation of a bipolar current system, the appearance of transient potential layers, and the carving of deep density cavities.

The work of F. S. Tsung and G. J. Morales is sponsored by ONR and NSF and that of J. N. Leboeuf by DOE. The original OSIRIS code was developed by Professor W. Mori's research group. The authors thank M. VanZeeland, W. Gekelman, S. Vincena, and G. Dimonte for valuable discussions about their experiment.

[1] K.-L. Klein, G. Trottet, P. Lantos, and J. P. Delaboudiniere, Astron. Astrophys. **373**, 1073 (2001).
[2] I. G. Richardson, E. W. Cliver, and H. V. Cane, Geophys. Res. Lett. **28**, 2569 (2001).
[3] R. E. Ergun, C. W. Carlson, J. P. McFadden, F. S. Mozer, L. Muschietti, I. Roth, and R. J. Strangeway, Phys. Rev. Lett., **81**, 826 (1998).
[4] K. Stasiewicz, and T. Potemra, J. Geophys. Res., **103**, 4315 (1998).
[5] A. N. Mostovych, B. H. Ripin, and J. A. Stamper, Phys. Rev. Lett. **62**, 2837 (1989).
[6] G. Dimonte and B. Remington, Phys. Rev. Lett. **70**, 1806 (1993).
[7] M. VanZeeland, W. Gekelman, S. Vincena, and G. Dimonte, Phys. Rev. Lett. **87**, 105001 (2001).
[8] F. Porcelli, E. Rossi, G. Cima, and A. Wootton, Phys. Rev. Lett., **82**, 1458 (1999).
[9] K. Stasiewicz, P. Bellan, C. Chaston, C. Kletzing, R. Lysak, J. Maggs, O. Pokhotelov, C. Seyler, P. Shukla, L. Stenflo, A. Streltsov, and J.-E. Wahlund, Space Sci. Rev. **92**, 423 (2000).
[10] R. G. Hemker, Ph.D. thesis, UCLA, 2000.
[11] J. Denavit, Phys. Fluids (1958–1988) **22**, 1384 (1979).
[12] T. Denelea and H. Urbassek, Phys. Plasmas **9**, 3209 (2002).
[13] A. V. Gurevich, L. V. Pariiskaya, and L. P. Pitaevskii, Sov. Phys. JETP **22**, 449 (1966).
[14] C. Melzer, S. Nunomura, D. Samsonov, Z. W. Ma, and J. Goree, Phys. Rev. E **62**, 4162 (2000).
[15] V. Nosenko, J. Goree, Z. W, Ma, and A. Piel, Phys. Rev. Lett. **88**, 135001 (2002).
[16] Recent experiments have verified the presence of ballistic electrons and correlated magnetic fields. W. Gekelman (private communications).
[17] C. C. Mitchell, J. E. Maggs, and W. Gekelman, Phys. Plasmas **9**, 2909 (2002).